Non-linear dendrites enable robust stimulus selectivity.

Romain D. Cazé *, **Sarah Jarvis,** * **Simon R. Schultz** *

*Centre for Neurotechnology and Department of Bioengineering, Imperial College London, South Kensington, London, SW7 2AZ, UK

Submitted to Proceedings of the National Academy of Sciences of the United States of America

Hearing, vision, touch – underlying all of these senses is stimulus selectivity, a robust information processing operation in which cortical neurons respond more to some stimuli than to others. For vision, Hubel and Wiesel discovered that certain neurons respond selectively to elongated visual stimuli, and proposed an elementary linear model to account for this selectivity. Recent experiments have however cast doubt on some aspects of this textbook model. Hyperpolarising a neuron can abolish selectivity in the soma, while selectivity in the dendrites - the receptive compartments of neurons - remains unaffected. A model assuming linear summation of inputs, like the Hubel and Wiesel model, cannot explain this observation. Here instead we employ a morphologically realistic model, incorporating non-linear dendrites reconstructed from real neurons, to implement stimulus selectivity. We show that this model explains the effect of hyperpolarisation, and implements stimulus selectivity more robustly than the classic model. It can remain selective even if 50% of its synapses fail. This demonstrates that in addition to increasing neuronal computational capacity, dendrites can also increase the robustness of neuronal computation. We also predict that a neuron that is initially stimulus non-selective can become selective when depolarized. This prediction stimulates new experimental studies on stimulus selectivity.Moreover, the robustness of our implementation provides a starting point for the development of fault-resistant neuromorphic chips.

Dendrites | stimulus selectivity | electrophysiology | single neuron computation

Over 50 years ago, Hubel and Wiesel discovered a canonical example of stimulus selectivity [1], the selectivity of striate cortical neuronal responses to bar-like visual stimuli of a particular spatial position and orientation. They proposed a model to account for this, in which simple cells develop orientation tuning through pooling of inputs aligned along a preferred axis, and complex cells linearly summate inputs from simple cells with the same orientation. Recently, however, several groups using two photon calcium imaging combined with whole cell patch clamp electrophysiology have presented data in apparent discordance with this model. Firstly, it was observed that the soma and dendrites of layer 2/3 cortical pyramidal cells show different tuning, with inputs sharing the same orientation preference distributed widely throughout the dendritic tree, and inputs with different orientation preferences interspersed within a dendritic locality [2]. In contrast, the Hubel and Wiesel complex cell would be expected to integrate inputs with a relatively narrow range of orientations. Secondly, it was observed that hyperpolarisation can eliminate orientation selectivity at the soma, while leaving the selectivity of dendrites unaffected [2, 3]. This disruption of somatic selectivity has also been observed in other sensory modalities such as touch [9], and thus may reveal a general principle underlying cellular information processing. A linear synaptic integration model such as the Hubel and Wiesel model would predict that the sub-threshold membrane potential remains stimulus selective.

Inputs with different orientation preferences are interspersed within the same dendritic locality might potentially be reconciled with the Hubel and Wiesel model, if simple cell inputs encoding the preferred stimulus make the highest number of or the strongest contacts. That hyperpolarisation eliminates orientation selectivity at the soma while leaving the dendrites unaffected, however, is difficult or impossible to reconcile with a linear synaptic integration model. How might it be explained? Here, we demonstrate that nonlinear integration in dendrites may provide a possible explanation.

Dendrites can enhance the computational capacity of single neurons. This stems from local and non-linear interactions of synaptic inputs in dendrites: the somatic depolarization resulting from multiple synaptic inputs can be larger (supralinear) [10] or smaller (sublinear) [11, 12, 13, 10] than their arithmetic sum. Either of these non-linearities endow neurons with greater computational capacity than expected from a linear model [8]. We therefore examined how stimulus selectivity could be incorporated into a biophysical neuron model by the use of nonlinear dendrites.

Non-linear interaction between synapses in the dendrites makes our neuron model sensitive to the spatial distribution of synaptic activity. We exploited this property to make our model stimulus selective (Fig. 1A). We reproduced the observation that dendritic selectivity can differ from somatic selectivity (Fig. 1B) by shaping of the spatial distribution of synapses (Fig. 1C). We placed 8 sets of 7 groups of 1 to 5 AMPA/NMDA-type synapses at 8x7 locations either scattered on 7 distinct primary dendrites or clustered on a single branch from a morphological reconstruction of a layer 2/3 stellate cell neuron [2] (Fig. 1D). The activation of a single synapse per location results in a somatic depolarization of 1 mV, independent of synapse location, as observed in [14] (Fig. 1E). We enforced this "dendritic democracy" [15] by scaling the synaptic conductance. Interestingly, these synapses interact

Significance

From the stripes of your shirt to the sound of your grandmother's name, your neurons are capable of selecting among stimuli. How do they perform this selection? The standard model assumes that a neuron receive the highest number of active inputs for its preferred stimulus. While this can explain many observations, it fails to address recent evidence that increasing the spike threshold abolishes stimulus selectivity. Here we propose an alternate model for stimulus selectivity which incorporates dendrites, the neuron's antenna for receiving inputs. Selective neurons in our model are more resilient to loss of synaptic inputs. Due to this increased robustness, our study paves the way for a new generation of fault-resistant neuromorphic chips.

Significance Statement

non-linearly in two distinct ways. When the activation of 7 synapses (1 per location) is clustered on a branch within (typically) 40 μm, they can generate a depolarization larger than their arithmetic sum at the soma because of the voltage-gated magnesium block of the NMDA current [16](Fig. 1E top black trace). In contrast, when 35 clustered synapses (5 per location) are active they interact sub-linearly, and the resulting voltage is smaller than the arithmetic sum, due to saturation [17, 18] (Fig. 1E bottom black trace). For scattered synapses, the interactions have the opposite behavior (Fig. 1E red trace), and the result is a more linear integration, as observed experimentally [19]. Therefore, the non-linear interaction between synapses depends on their spatial distribution and on the number of active synapses: For 35 active synapses, clustered synapses interact sub-linearly whereas scattered synapses interact almost linearly (Fig. 1F). This demonstrates that synaptic integration in a realistic reconstruction of a layer 2/3 neuron is highly sensitive to the spatial distribution of active synapses, and even a few synapses can effectively depolarize the cell when active synapses are spatially dispersed throughout the dendrites. We exploited this sensitivity to the spatial distribution of synapses to generate stimulus selectivity. In our model, only the population coding for the preferred stimulus makes functional synapses on all the 7 different primary dendritic branches, whereas the populations coding for non-preferred stimuli each synapse on a single branch. In this case, a single NMDA spike is generated and is, in most cases, insufficient to make the neuron spike. Conversely, for the preferred stimulus the neuron fires because multiple NMDA spikes are generated in parallel, as observed *in vitro* [20] and *in vivo* [21, 22] (Fig. 2A). Both scenarios are illustrated in animations provided as supplementary material (see movies S1 and S2).

Hyperpolarization abolishes selectivity at the soma both in experiments and in our model (Fig. 2A). Injecting 100pA into the neuron changes its resting membrane potential, pulling the somatic membrane potential down to -95mV from -64mV. The neuron stops firing action potentials, however hyperpolarisation also affects the shape of the subthreshold potential in our non-linear model. This modification of the voltage range changes how the synapses interact. When we hyperpolarise the neuron, the depolarization difference between the scattered and clustered situation decreases and becomes negligible (Fig. 2C). Consequently, there is very little difference in the depolarization induced by the preferred and non-preferred stimuli, and somatic stimulus selectivity is lost (Fig. 2B and C). Conversely, stimulus selectivity in dendrites remains sharp under hyperpolarisation, because it depends instead upon the non-linearity of integration across NMDA synapses, which is retained under hyperpolarisation (Fig. 1B). We conclude that the sensitivity to the spatial distribution of synapses can explain the effect of hyperpolarisation on somatic selectivity.

Our implementation of stimulus tuning is possible only if synaptic integration is locally non-linear, and impossible if integration is completely linear. If the model is linear, the position of synapses relative to each other becomes irrelevant and it is impossible to use the spatial distribution of synapses to implement stimulus selectivity. Our theoretical framework is sufficient to explain the experimental observations: While a neuron might instead use a different non-linear mechanism than the one we have assumed, we show that a sublinear dendritic non-linearity is sufficient.

In the biophysical model, we used relatively few synapses (280) and we placed these synapses in a non-random fashion. Relaxing these two non-realistic assumptions, by using an abstract non-linear model with 4600 synapses distributed almost randomly. This enabled us to study the more general case of a biologically realistic order of magnitude.

We found that using the spatial distribution of synapses in a non-linear model adds robustness against both synaptic failure and the loss of dendrites (Fig. 3). To show that, we computed the depolarization using our non-linear model, and scaled up our implementation to include more than 4000 synapses. We used 8 ensembles of presynaptic neurons, with each ensemble coding for a different stimulus. The ensemble coding for the preferred stimulus targeted all dendritic compartments randomly, whereas the ensembles coding for non-preferred stimuli each tended to cluster their synapses on a different dendritic compartment (30%). Their remaining synapses distributed randomly. We found this difference in spatial distribution to be sufficient to create stimulus selectivity. On the one hand, the preferred stimulus can make in this model up to 200 fewer synapses than the non-preferred stimuli without altering stimulus selectivity (Fig. 3A); on the other hand, in a linear model it is necessary that the preferred stimulus makes the highest number of contacts (for proof, see Methods). Moreover, a neuron can be stimulus selective even if input sources coding for the non-preferred stimuli cluster only 10% of their synapses (Fig. 3B). These properties confer robustness against synaptic failure or the loss of dendrites (Fig. 3C to F). We first study examples: We either randomly made 50% of input sources fail in a non-linear (Fig. 3C and D) or a linear model (Fig. 3F), or two dendrites (Fig. 3E), and look at the effect on the discrimination ability - the separability - between preferred from non-preferred stimuli. We observed that despite synaptic failure, the two types of stimuli in a non-linear model still generate distinct depolarizations at the soma (Fig. 3D); this was also the case when we removed two dendrites (Fig. 3E). This shows that a neuron suffering from synaptic failure or dendritic loss can remain selective by adjusting its somatic spike threshold during a recovery period. On the contrary, for a model where integration is linear, the preferred and non-preferred stimuli can no longer be discriminated when sources encoding the preferred direction lose too many synapses and are no longer the ensemble with the highest number of synaptic contacts. In Fig. 3F, we systematically compare the linear and the compartimentalized non-linear model. From this, we conclude that implementations using the spatial distribution of synapses are more robust to synaptic failure than implementations which make use of linear synaptic integration.

In summary, we have demonstrated that local and non-linear synaptic integration enables neurons to implement robust stimulus selectivity. Our non-linear model, as an alternative to linear synaptic integration models based upon the principles established by Hubel and Wiesel, can generate stimulus selectivity and reproduce two recent and relatively surprising experimental observations: i) complex cells receive inputs coding for a variety of stimuli [2, 3] (Fig. 1); and ii) hyperpolarisation disrupts selectivity at the soma [2, 9] (Fig. 2) while leaving dendritic selectivity unimpaired. We demonstrated that this implementation of stimulus selectivity in a layer 2/3 biophisycal model is more robust than an equivalent model with linear synaptic integration (Fig. 3).

The additional robustness of our model comes from local and non-linear synaptic integration. This type of integration can make a neuron cluster sensitive, but our model is, in this study, instead scatter sensitive. Sensitivity to scatter in the spatial distribution of active synapses has previously been described [23], but never exploited computationally. Our results were strongly motivated by experimental results on the spatial distribution of orientation preferences with the dendritic tree reported by [2], supported by results from related studies

[3, 9]. We consider that there is a strong need for additional experimental work on the distribution of sensory tuning properties within the dendritic tree of neurons across a number of cortical areas. We note that our implementation of stimulus specificity is compatible with a bias in synaptic connectivity, where the strongest input comes from the preferred stimulus, as observed recently by Chen et al [24].

Our results, taken together, make two additional testable predictions. Firstly, they predict that a neuron may recover its tuning after losing a large fraction of either its synapses or dendrites, due to the robustness behaviour displayed here. Secondly, the model predicts that a neuron in a sensory cortical area with no apparent stimulus tuning can acquire stimulus selectivity when depolarized. A similar phenomenon is observed in place cells [25].

In this study we considered the sensitivity of a layer 2/3 complex cell to the orientation of a visual stimulus. One important feature of the complex cell is its phase insensitivity - which is frequently accounted for by integrating inputs from simple cell receptive fields in quadrature [26]. It would be interesting to explore whether inputs sensitive to different phases cluster in nearby dendritic locations, or are scattered throughout the dendritic tree. Thus far, the spatial distribution of phase sensitivity within the dendritic tree of visual cortical neurons is yet to be characterised, however, based on the phase insensitivity of the complex cell we might expect inputs tuned for similar spatial phase to be scattered widely amongst the dendritic tree, rather than clustered on particular dendrites. A specific prediction here would be that the degree of scatter of spatial phase amongst the dendrites would correlate with the "complexity" of the cell, as measured by the ratio between the DC and first harmonic of the stimulus modulated response.

Our nonlinear dendritic integration will inform the design of neuromorphic chips, as it suggests that the use of dendrites - even if passive- can extend the robustness of the circuit, as well as adding information processing capacity. Dendrites may not only increase the computational power of each unit, but also increase their resilience, addressing a crucial issue in the design of fault-tolerant chip architectures. While we have demonstrated these capabilities in the context of a neuron's stimulus selectivity to a visual stimulus, the model we have proposed is general, and potentially reflects a canonical computational principle for neuronal information processing.

Materials and Methods

Biophysical model. For detailed modelling, we used a reconstructed morphology of a stellate cell from Layer 2/3 of visual cortex in mouse [2]. The axial resistance in each section was $R_a = 35.4\Omega$, and passive elements were included ($g_l = 0.001\Omega^{-1}$, $e_l = -65$ mV). Spiking was implemented using a hard threshold of -45mV giving the same result but more realistic [31] than a Hodgkin-Huxley model (data not show), whereupon we set the voltage to 20mV in the following timestep before resetting at -65mV. The model was implemented using NEURON with a Python wrapper [27], with the time resolution set to 0.1ms.

Synaptic inputs. We generated 280 presynaptic neurons divided into 8 sets of 35 neurons, corresponding to 8 different orientations. Each had a background firing rate of 1 Hz which increased to 10Hz during the presentation of the stimulus. As experimental evidence suggests that stimulus information is coded not only by an increase in firing rate but also in spike-time correlation [28, 29], we inserted 20 synchronous spikes to the spiketrains from neurons encoding the preferred stimulus, raising their firing rate to 30 Hz.

Conductance based NMDA-type synapses. NMDA-like inputs were included by modelling voltage-dependent, conductance-based synapses that generated postsynaptic currents $i_s = g(t)g_{\rm mg}(v)\times(v(t)-e_s)$, with reversal potential e_s =0 mV. For $g(t)$, we used an alpha-function with rise and decay time constants $\tau_1 = 0.1$ms and $\tau_2 = 10$ms respectively. Values for τ_1 and τ_2 were chosen to be deliberately lower than those for real glutamate binding on NMDA channels to account for the presence of voltage-gated calcium dependent potassium channels in the membrane. The voltage-dependent conductance $g_{mg}(v)$ was determined following the formalism in [30] and assuming $[{\rm Mg}^{2+}]$ =1mM.

Multi-compartmental model. Our multi-compartmental model consists of 7 dendrites, each which receives input from 8 groups presynaptic neurons corresponding to 8 different orientations (Fig. 4). Here, the preferred stimulus (0 degrees) projects 700 synapses randomly distributed across all 7 dendrites. In contrast, non-preferred stimuli make 650 connections each, with the mean number of synaptic contacts for each stimulus-dendritic pair described in Table 1, including a bias such that 40% of input from each orientation preferentially target one of the dendrites and the remaining 60% being evenly distributed among the remaining 6 dendrites. Additionally, clustering biases were generated by keeping the 40% bias from a given stimulus, and supplying the specified clustering bias additionally from the remaining 60% of inputs. A dendrite saturates when 100 of its synapses are active, and the somatic output is determined as the arithmetic sum of all the dendritic output.

A necessary condition for the linear model. The highest weight needs to be from the preferred stimulus in a linear model. To prove that let us consider the simplest scenario where two presynaptic neurons each synapse onto a postsynaptic neuron. We arrange it so that one input codes for the preferred stimulus while the other for a non-preferred stimulus, and $W_{\rm pref}$ and $W_{\rm nonpref}$ be the amplitude of their resulting depolarization on the postsynaptic neuron. Here, stimulus selectivity is possible only if $W_{\rm pref} \geq \Theta$ and $W_{\rm nonpref} < \Theta$, which is equivalent to $W_{pref} > \Theta > W_{\rm nonpref}$. This condition can be generalized for any number of presynaptic neurons, and implies in the linear neuron model when constrained to positive values of W that stimulus selectivity is only possible when the preferred stimulus has the highest weight.

ACKNOWLEDGMENTS. The authors thank Dr Hongbo Jia for providing the layer 2/3 complex cell reconstruction used for the model presented in this paper, and Dr. Andrew Gallimore, Dr. Mark Humphries, Dr. Amanda Foust, Dr. Boris Gutkin, Dr. Fleur Zeldenrust, Dr Matthijs Van Der Meer for their comments on the draft manuscript. This work was supported by EU FP7 Marie Curie Initial Training Network 289146 (NETT). SJ is supported by EU FP7 Marie Curie fellowship (PIEF-GA-2013-628086), and SRS by a Royal Society Industry Fellowship.

1. Hubel, D. H. & Wiesel, T. N. Receptive fields of single neurones in the cat's striate cortex. The Journal of Physiology 148, 574–591 (1959).
2. Jia, H., Rochefort, N. L., Chen, X. & Konnerth, A. Dendritic organization of sensory input to cortical neurons in vivo. Nature 464, 1307–1312 (2010).
3. Smith, S. L., Smith, I. T., Branco, T. & Häusser, M. Dendritic spikes enhance stimulus selectivity in cortical neurons in vivo. Nature 503, 115–20 (2013).
4. Zador, A. A. M., Claiborne, B., Brown, T. T. H. & Clairborne, B. J. Nonlinear pattern separation in single hippocampal neurons with active dendritic membrane. Advances in neural information processing systems 51–51 (1993).
5. Agmon-Snir, H., Carr, C. & Rinzel, J. The role of dendrites in auditory coincidence detection. Nature 393, 268–272 (1998).
6. Poirazi, P., Brannon, T. & Mel, B. Pyramidal neuron as two-layer neural network. Neuron 37, 989–999 (2003).
7. Cazé, R. D., Humphries, M. & Gutkin, B. S. Spiking and saturating dendrites differentially expand single neuron computation capacity. Advances in neural information processing systems 25, 1–9 (2012).
8. Cazé, R. D., Humphries, M. & Gutkin, B. Passive Dendrites Enable Single Neurons to Compute Linearly Non-separable Functions. PLoS Computational Biology 9 (2013).
9. Lavzin, M., Rapoport, S., Polsky, A., Garion, L. & Schiller, J. Nonlinear dendritic processing determines angular tuning of barrel cortex neurons in vivo. Nature 490, 397–401 (2012).
10. Polsky, A., Mel, B. W. & Schiller, J. Computational subunits in thin dendrites of pyramidal cells. Nature Neuroscience 7, 621–627 (2004).
11. Tamás, G., Szabadics, J. & Somogyi, P. Cell type- and subcellular position-dependent summation of unitary postsynaptic potentials in neocortical neurons. Journal of Neuroscience 22, 740–747 (2002).
12. Abrahamsson, T., Cathala, L., Matsui, K., Shigemoto, R. & DiGregorio, D. A. Thin Dendrites of Cerebellar Interneurons Confer Sublinear Synaptic Integration and a Gradient of Short-Term Plasticity. Neuron 73, 1159–1172 (2012).
13. Cash, S. & Yuste, R. Input summation by cultured pyramidal neurons is linear and position-independent. The Journal of Neuroscience 18, 10–15 (1998).

14. Smith, M., Ellis-Davies, G. & Magee, J. Mechanism of the distance-dependent scaling of Schaffer collateral synapses in rat CA1 pyramidal neurons. The Journal of Physiology 548, 245 (2003).
15. Häusser, M. Synaptic function: Dendritic democracy. Current Biology 11, R10–R12 (2001).
16. Nevian, T., Larkum, M., Polsky, A. & Schiller, J. Properties of basal dendrites of layer 5 pyramidal neurons: a direct patch-clamp recording study. Nature 200, 7 (2007).
17. Koch, C., Poggio, T. & Torres, V. Retinal ganglion cells: a functional interpretation of dendritic morphology. Phil. Trans. R. So. Lond. B 298, 227–263 (1982).
18. Tran-van Minh, A. et al. Contribution of sublinear and supralinear dendritic integration to neuronal computations. Frontiers in Cellular Neuroscience 9, 1–15 (2015).
19. Jia, H., Varga, Z., Sakmann, B. & Konnerth, A. Linear integration of spine Ca2+ signals in layer 4 cortical neurons in vivo. Proceedings of the National Academy of Sciences of the United States of America 111, 9277–82 (2014).
20. Larkum, M. E., Waters, J., Sakmann, B. & Helmchen, F. Dendritic spikes in apical dendrites of neocortical layer 2/3 pyramidal neurons. The Journal of Neuroscience 27, 8999–9008 (2007).
21. Hill, D. N., Varga, Z., Jia, H., Sakmann, B. & Konnerth, A. Multibranch activity in basal and tuft dendrites during firing of layer 5 cortical neurons in vivo. Proceedings of the National Academy of Sciences 110, 13618–13623 (2013).
22. Palmer, L. M. et al. NMDA spikes enhance action potential generation during sensory input. Nature Neuroscience 17, 383–90 (2014).
23. Mel, B. W. Synaptic integration in an excitable dendritic tree. Journal of Neurophysiology 70, 1086–101 (1993).
24. Chen, T.-W. et al. Ultrasensitive fluorescent proteins for imaging neuronal activity. Nature 499, 295–300 (2013).
25. Lee, D., Lin, B.-J. & Lee, A. K. Hippocampal place fields emerge upon single-cell manipulation of excitability during behavior. Science 337, 849–53 (2012).
26. Emerson, R. C., Bergen, J. R. & Adelson, E. H. Directionally selective complex cells and the computation of motion energy in cat visual cortex. Vision Research 32, 203–218 (1992).
27. Hines, M. L., Davison, A. P. & Muller, E. NEURON and Python. Frontiers in Neuroinformatics 3, 1 (2009).
28. Bruno, R. M. & Sakmann, B. Cortex is driven by weak but synchronously active thalamocortical synapses. Science 312, 1622–7 (2006).
29. DeCharms, R. C. & Merzenich, M. M. Primary cortical representation of sounds by the coordination of action-potential timing. Nature 381, 610–613 (1996).
30. Destexhe, a., Mainen, Z. F. & Sejnowski, T. J. An Efficient Method for Computing Synaptic Conductances Based on a Kinetic Model of Receptor Binding. Neural Computation 6, 14–18 (1994).
31. Brette, R. What Is The Most Realistic Single-Compartment Model of Spike Initiation? PloS Computational Biology 11, e1004114 (2015).

Table 1. Synapses distribution in multi-compartmental model. Mean number of synapses made by each presynaptic ensemble for each stimulus, for each postsynaptic dendrite.

	Dendrite (d_j)							
Preferred orientation	0	1	2	3	4	5	6	Total
0	100	100	100	100	100	100	100	700
45	260	65	65	65	65	65	65	650
90	65	260	65	65	65	65	65	650
135	65	65	260	65	65	65	65	650
180	65	65	65	260	65	65	65	650
225	65	65	65	65	260	65	65	650
270	65	65	65	65	65	260	65	650
315	65	65	65	65	65	65	260	650

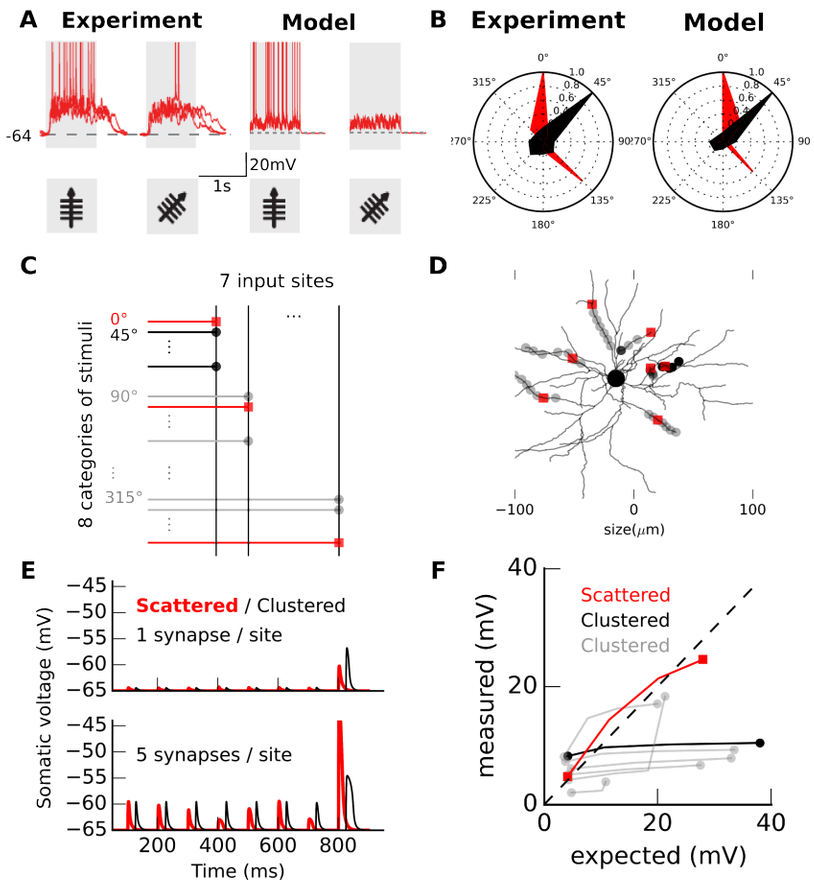

Fig. 1. Differential stimulus tuning of the soma and dendrites can arise from the spatial distribution of synapses. A Somatic response to two stimuli (0/45 degrees). Dotted horizontal lines indicate resting potential with shaded areas indicating stimulus presentation. **B**. Polar plots of somatic (red, normalized spike count) and an example of dendritic selectivity (black, normalized calcium signal integral in experiments or voltage integral in model). The chosen dendrite corresponds to the black color in all panels. **C** Schematic depiction of synapses' spatial distribution. Horizontal lines are axons color coded for their stimulus selectivity (red: preferred, black/gray: non-preferred). Vertical lines are distinct primary dendrites. Each dot corresponds to 5 synaptic contacts. **D** 2-D projection of a reconstructed layer 2/3 neuron from [2]. Dots are input locations color coded as in **C**. **E** Somatic depolarization when 1 synapse (top) or 5 synapses (bottom) are stimulated at each location from 0 to 800 ms; and when stimulation occurs at the 7 locations simultaneously from 800 to 1000 ms. Here we used two sets of locations (thick red line: scattered / thin black line: clustered). **F**. The expected depolarization based on arithmetic summation, versus that measured from the simulation, for 8 sets of 7 locations.

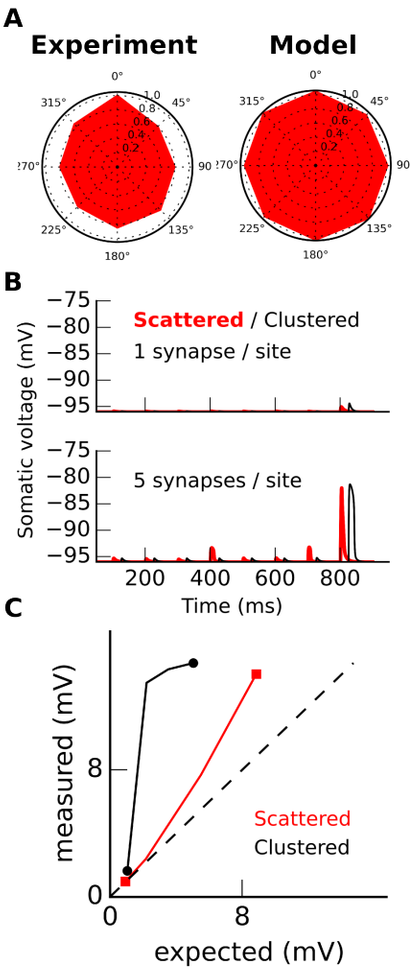

Fig. 2. Hyperpolarization disrupts stimulus selectivity at the soma. **A**. Polar plots of somatic stimulus tuning, given by the normalized spike count. Hyperpolarization induced by 100 pA both in the experiment and in our simulation. Experimental data replotted from [2]. **B** Somatic depolarization when 1 synapse (upper) or 5 synapses (lower) are stimulated at each location from 0 to 800 ms; and when stimulation occurs at the 7 locations simultaneously from 800 to 1000ms. We used the same sets of locations as in Fig. 1 (red: scattered/black: clustered). **C**. The expected depolarization based on the arithmetic sum of individual depolarizations versus the depolarization measured in the simulation. This is quantified for the 8 sets of 7 locations using the same color code as in Fig. 1.

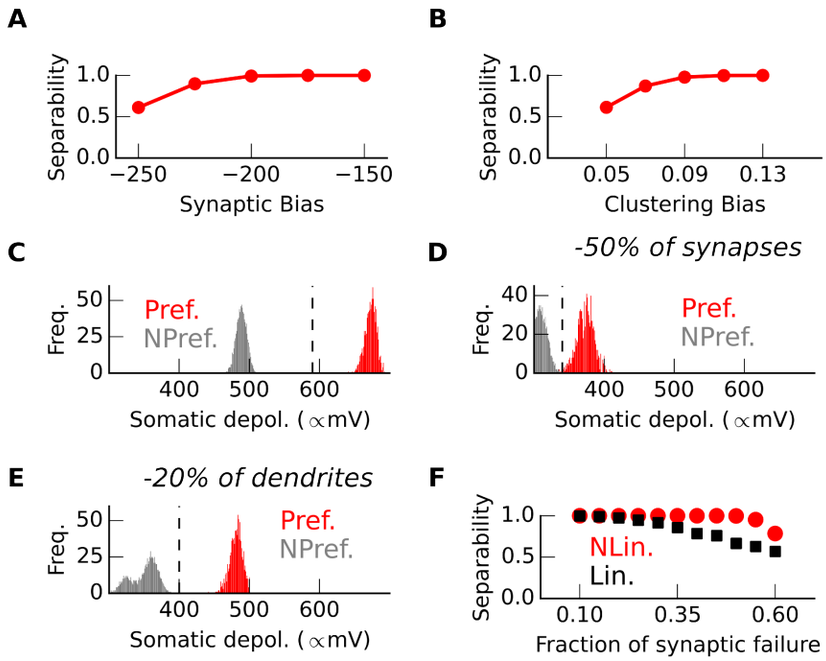

Fig. 3. Using the spatial distribution of active synapses for neuronal computation increases robustness to synaptic failure. We presented 8 input patterns to 1000 random instances of our model. Separability - the fraction of model instances able to separate preferred from non-preferred stimuli - is shown as a function of **A** the difference in the number of synapses between the fixed number of 700 preferred and a variable amount of non-preferred inputs (Synaptic Bias), and **B** the fraction of synapses from a non-preferred stimulus on each dendrite in addition to the baseline proportion originally obtained when uniformly distributed (Clustering Bias). **C** The probability distribution of the resulting somatic depolarization (arbitrary units proportional to mV) for all model instances after filtering in dendrites for either preferred (red) or non-preferred (gray) stimuli. Dendritic saturation here occurs at 100 units of depolarization. The vertical dotted line is the threshold that separates preferred from non-preferred inputs. **D** Depolarization distribution with 50% of synapses randomly removed for the two stimuli. **E** Depolarization distribution with 20% of synapses randomly removed. **F** Separability fraction for 1000 instances of the problem as a function of the fraction of synaptic failures. Red circles: non-linear model; Black squares: linear model.

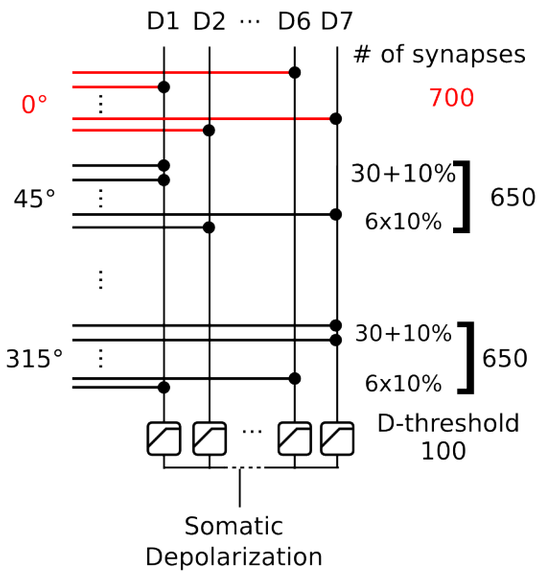

Fig. 4. Using the spatial distribution of synapses to implement stimulus selectivity. Each horizontal line represents an axon coming from a presynaptic neuron. Red lines correspond to the population activated for the preferred stimulus. Each vertical line represents a different dendrite.